doi:10.1093/jmcb/mjy068
Published online November 14, 2018

Article

Zebrafish *hhex*-null mutant develops an intrahepatic intestinal tube due to de-repression of *cdx1b* and *pdx1*

Ce Gao[1,†], Weidong Huang[1,†], Yuqi Gao[1], Li Jan Lo[1], Lingfei Luo[2], Honghui Huang[2], Jun Chen[3], and Jinrong Peng[1,*]

[1] MOE Key Laboratory for Molecular Animal Nutrition, College of Animal Sciences, Zhejiang University, 866 Yu Hang Tang Road, Hangzhou 310058, China
[2] College of Life Sciences, Southwest University, Chongqing 400715, China
[3] College of Life Sciences, Zhejiang University, 866 Yu Hang Tang Road, Hangzhou 310058, China
[†] These authors contributed equally to this work.
[*] Correspondence to: Jinrong Peng, E-mail: pengjr@zju.edu.cn

Edited by Anming Meng

The hepatopancreatic duct (HPD) system links the liver and pancreas to the intestinal tube and is composed of the extrahepatic biliary duct, gallbladder, and pancreatic duct. Haematopoietically expressed-homeobox (Hhex) protein plays an essential role in the establishment of HPD; however, the molecular mechanism remains elusive. Here, we show that zebrafish *hhex*-null mutants fail to develop the HPD system characterized by lacking the biliary marker Annexin A4 and the HPD marker *sox9b*. The hepatobiliary duct part of the mutant HPD system is replaced by an intrahepatic intestinal tube characterized by expressing the intestinal marker *fatty acid-binding protein 2a* (*fabp2a*). Cell lineage analysis showed that this intrahepatic intestinal tube is not originated from hepatocytes or cholangiocytes. Further analysis revealed that *cdx1b* and *pdx1* are expressed ectopically in the intrahepatic intestinal tube and knockdown of *cdx1b* and *pdx1* could restore the expression of *sox9b* in the mutant. Chromatin-immunoprecipitation analysis showed that Hhex binds to the promoters of *pdx1* and *cdx1b* genes to repress their expression. We therefore propose that Hhex, Cdx1b, Pdx1, and Sox9b form a genetic network governing the patterning and morphogenesis of the HPD and digestive tract systems in zebrafish.

Keywords: liver development, hepatopancreatic duct (HPD), *hhex*, *pdx1*, *cdx1b*

Introduction

Organogenesis of the zebrafish digestive system is a dynamic process that starts from 26 hours post-fertilization (hpf) and gives rise to morphologically distinctive organ buds at around 54 hpf, followed by organ growth and maturation stages (Field et al., 2003b; Zaret, 2008; Goessling and Stainier, 2016). During the 26–54 hpf time window, hepatoblasts and pancreatic precursor cells are first differentiated from the endodermal rod and finally form a discrete liver and pancreatic bud, respectively (Field et al., 2003b; Huang et al., 2008; Tao and Peng, 2009). The liver bud, gallbladder, and pancreatic bud are linked by a ductal network named as the hepatopancreatic duct (HPD) system that finally opens through the hepatopancreatic ampulla to the intestinal tract to become part of the digestive system (Dong et al., 2007; Delous et al., 2012; Manfroid et al., 2012). Extensive work has been carried out to study the organogenesis of the liver and pancreas and a number of regulatory factors have been identified (Zaret, 2008; Shih et al., 2013; Goessling and Stainier, 2016). In contrast, only a few factors have been identified to specify the HPD. For example, *sox9b* is found to be an essential gene for specifying HPD (Delous et al., 2012; Manfroid et al., 2012), and Fgf10 to be a key signaling molecule for patterning and differentiation of the HPD system (Dong et al., 2007). Molecular marker staining has revealed that the identity of HPD cells is clearly distinct from but is related to the hepatoblasts and pancreatic precursor cells. For example, HPD cells are characterized to be Annexin A4- and Sox9b-positive cells (Dong et al., 2007; Delous et al., 2012; Manfroid et al.,

Received October 1, 2018. Accepted November 13, 2018.

2012; Zhang et al., 2014). Although the relationship between HPD cells and hepatic or pancreatic cells in zebrafish has been investigated in several cases, the relationship between HPD cells and intestinal epithelium is hardly investigated.

Haematopoietically expressed-homeobox (Hhex), also known as proline-rich homeodomain (PRH), is a homeobox-type transcriptional factor that was first identified in the avian and human haematopoietic and liver cells (Crompton et al., 1992; Hromas et al., 1993). Later studies showed that Hhex plays important roles in cell proliferation and differentiation (Soufi and Jayaraman, 2008). Hhex is involved in regulating the development of blood cells (Paz et al., 2010; Goodings et al., 2015), liver (Bort et al., 2006; Rankin et al., 2011; Watanabe et al., 2014), pancreas (Bort et al., 2004; Zhao et al., 2012), and heart (Hallaq et al., 2004; Liu et al., 2014) in different species. Regarding the role of Hhex in the development of the HPD system, Bort et al. found that Hhex-positive progenitors in the $Hhex^{LacZ/LacZ}$ null mice conferred a duodenal-like cell fate (Bort et al., 2006). Hunter and colleagues observed that deletion of Hhex in the hepatic diverticulum (*Foxa3-Cre;*$Hhex^{d2,3/-}$) resulted in a small and cystic liver together with absence of the gallbladder and the extrahepatic bile duct (Hunter et al., 2007), demonstrating that Hhex is required the hepatobiliary development in mice. Importantly, their anatomic evidence showed that the extrahepatic biliary duct is replaced by duodenum in *Foxa3-Cre;*$Hhex^{d2,3/-}$ mouse embryos (Hunter et al., 2007). Recent studies have shown that Hhex can direct the differentiation of stem cells to hepatocytes (Kubo et al., 2010; Arterbery and Bogue, 2016). Hhex fulfills its function by regulating the expression of a number of downstream genes (Cong et al., 2006; Williams et al., 2008; Watanabe et al., 2014) and itself is regulated by factors including HNF3β, Smad, Wnt, and Sox17 signaling (Denson et al., 2000; Zhang et al., 2002; Rankin et al., 2011; Liu et al., 2014). Mutation in *hhex* is associated with certain human diseases (Shields et al., 2016).

In zebrafish, morpholino-mediated gene knockdown showed that *hhex* is essential for liver and pancreas development (Wallace et al., 2001). In addition to its expression in the liver and pancreatic bud, *hhex* is also highly expressed in the HPD precursor cells, displaying a similar dynamic expression patterns as in mice (Bogue et al., 2000; Bort et al., 2004), suggesting a role of Hhex in the development of HPD in zebrafish. In this report, by studying zebrafish *hhex* null mutants, we find that loss-of-function of Hhex leads to the formation of an intrahepatic intestinal tube at the expense of organogenesis of the HPD system. Molecular study reveals that Hhex represses the expression of *caudal-related homeobox 1b (cdx1b)* and *pancreatic and duodenal homeobox 1 (pdx1)* to safeguard the cell identity and morphogenesis of the HPD system.

Results

Loss-of-function of hhex leads to abnormal liver and exocrine pancreas development

In zebrafish, hepatic and pancreatic differentiations are characterized by thickening of the foregut endoderm at around 28hpf (Ober et al., 2003; Huang et al., 2008; Tao and Peng, 2009; Goessling and Stainier, 2016). We performed a WISH to check the expression of *hhex* at 28hpf and found that the *hhex* transcripts were detected in the prospective liver bud and pancreatic bud (Figure 1A). The zebrafish genome contains a single copy of the *hhex* gene located on chromosome 12 (Figure 1B, upper panel). To generate *hhex*-knockout mutants, we designed a guide-RNA (gRNA) based on the sequence of the exon 1 of the *hhex* gene (Figure 1B, lower panels) and co-injected *hhex*-specific gRNA with *Cas9* mRNA into one-cell stage embryos. The efficiency of *hhex*-gRNA in the injected embryos was about ~40% (Supplementary Figure S1A). F1 progenies were screened for *hhex* mutants and two independent deletion alleles were obtained, with one deleted 17 bp ($hhex^{zju1}$ allele) and another 11 bp ($hhex^{zju2}$ allele) in the exon 1 of *hhex* (Figure 1C). Each of these two alleles causes a frame-shift to the open reading frame (ORF) of *hhex* and introduces an early stop codon to disrupt the translation of *hhex* (Supplementary Figure S1B), suggesting that both are likely null alleles.

To check the digestive organs development in $hhex^{zju1}$, we performed WISH using the *fabp10a* (liver marker), *trypsin* (exocrine pancreas marker), *fabp2a* (intestine marker), and *insulin* (islet marker) probes, on the wild-type (WT) and $hhex^{zju1}$ embryos at 3 days post-fertilization (dpf). The result showed that the $hhex^{zju1}$ mutant displays a small liver phenotype and is absent of a detectable exocrine pancreas (Figure 1D), while the development of the intestine and islet was not obviously affected (Figure 1D). To determine the time point when the mutant phenotype is discernable, we performed WISH using pan-endodermal markers *foxa3* and *gata6* and early hepatic marker *prox1*. We found that the initiation of the liver primordium appeared to be normal in the $hhex^{zju1}$ mutant at 30- and 34-hpf as revealed by these molecular markers (Figure 1E). However, by 48hpf, the growth of the liver bud appeared to be retarded in the $hhex^{zju1}$ mutant (Figure 1E). The $hhex^{zju2}$ mutant also displayed a small liver and undetectable exocrine pancreas phenotype (Supplementary Figure S1C). Therefore, as observed in the *hhex*-conditional-knockout mice (Bort et al., 2006; Hunter et al., 2007), Hhex is essential for the outgrowth of the liver bud but not specification of the hepatic cells.

Generation of the Tg(bhmt:EGFP) reporter fish that faithfully recapitulates the expression pattern of the endogenous bhmt

The transgenic reporter fish *Tg(fabp10a:DsRed;elastase:GFP)* is frequently used in the liver development study (Dong et al., 2007). However, due to the fact that the expression of *fabp10a* is only weakly detectable at around 48hpf (Her et al., 2003), it is desirable, especially in the case of studying liver development in $hhex^{zju1}$, to obtain a reporter line that can robustly indicate the liver development before 48hpf. The *betaine homocysteine S-methyltransferase* (*bhmt*) is strongly expressed in the liver primordium in 34hpf-old zebrafish embryos (Yang et al., 2011). The zebrafish genome contains a single copy of the *bhmt* gene located on chromosome 21 (Figure 2A, upper panel). A genomic DNA fragment 5.2 kb upstream of the translation start codon

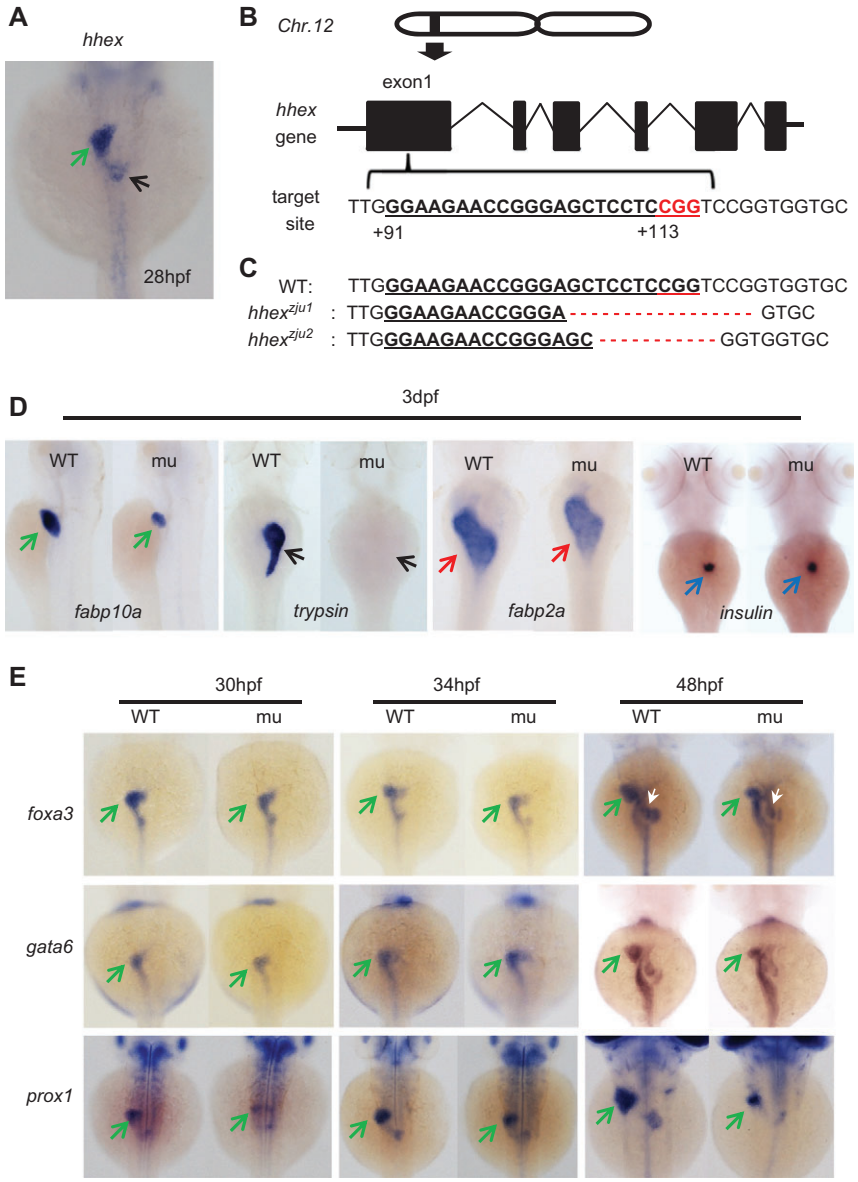

Figure 1 *hhex*^{zju1} confers a small liver and pancreas phenotype. (**A**) WISH showing the expression pattern of *hhex* in a representative embryo at 28hpf. (**B**) Diagrams showing the chromosome position (upper panel) and genomic structure (middle panel) of *hhex*. Bottom panel: the gRNA target sequence (+91 to +113 from the start codon ATG of *hhex*). (**C**) Sequence alignment showing the 17 bp and 11 bp deletion in *hhex*^{zju1} and *hhex*^{zju2}, respectively. (**D**) WISH using *fabp10a*, *trypsin*, *fabp2a*, and *insulin* probes on embryos at 3dpf. (**E**) WISH using *foxa3*, *gata6*, and *prox1* probes on WT and *hhex*^{zju1} mutant at 30hpf, 34hpf, and 48hpf. WT, wild-type; mu, *hhex*^{zju1}; green arrow, liver bud; black arrow, exocrine pancreas; red arrow, intestinal tube; blue arrow, islet; white arrow, swimming bladder.

ATG of *bhmt* was amplified by PCR using primer pair *bhmt* promoter (Supplementary Table S1). This DNA fragment was cloned into pEGFP-1 upstream of the *EGFP* gene to generate the *bhmt:EGFP* plasmid which was then injected into one-cell stage embryos (Figure 2A, lower panel). The *Tg(bhmt:EGFP)* transgenic fish was obtained from the progenies of the injected embryos. In *Tg(bhmt:EGFP)*, EGFP signal was detected in the liver primordium at 32hpf (Figure 2B, outlined by dashed lines), and in the liver bud at 2dpf, 3dpf, 4dpf, 5dpf, and 6dpf. EGFP is also detected in the yolk syncytial layer (YSL), but is specifically restricted in the liver at 6dpf when the yolk is fully absorbed (Figure 2B). In the *Tg(bhmt:EGFP)* background, we performed immunostaining of Bhmt in the cryosections obtained from the embryos at 32hpf, 2dpf, 4dpf, and 6dpf. The result showed that the EGFP signal is fully co-localized with the Bhmt signal in the liver and YSL (Figure 2C). Therefore, the expression pattern of EGFP in *Tg(bhmt:EGFP)* faithfully recapitulates the expression pattern of the endogenous *bhmt* gene.

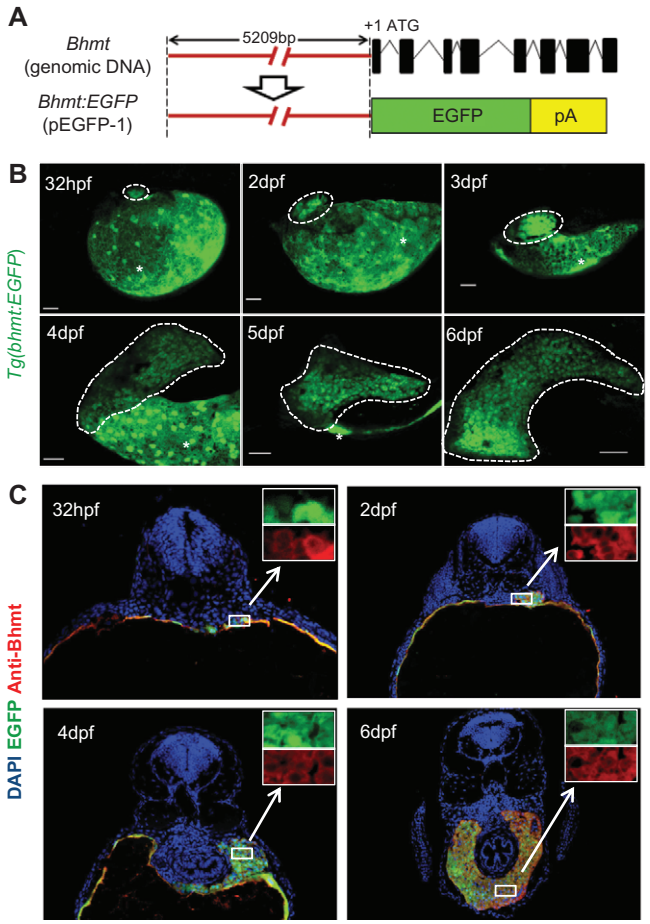

Figure 2 *Tg(bhmt:EGFP)* recapitulates the expression pattern of the endogenous *bhmt*. (**A**) Diagrams showing the genomic structure of *bhmt* (upper panel) and the *bhmt:EGFP* construct (lower panel). A 5209-bp DNA fragment upstream of the start codon of *bhmt* is cloned upstream of the reporter gene *EGFP*. pA, poly A. (**B**) Examining the expression pattern of Egfp in *Tg(bhmt:EGFP)* at 32hpf, 2dpf, 4dpf, and 6dpf. The liver region is circulated with a dashed line. *Yolk. (**C**) Co-immunostaining of EGFP (in green) and the endogenous Bhmt (in red) in *Tg(bhmt:EGFP)* at 32hpf, 2dpf, 4dpf, and 6dpf. The insets represent the high magnification view of the boxed regions. DAPI: nuclei staining.

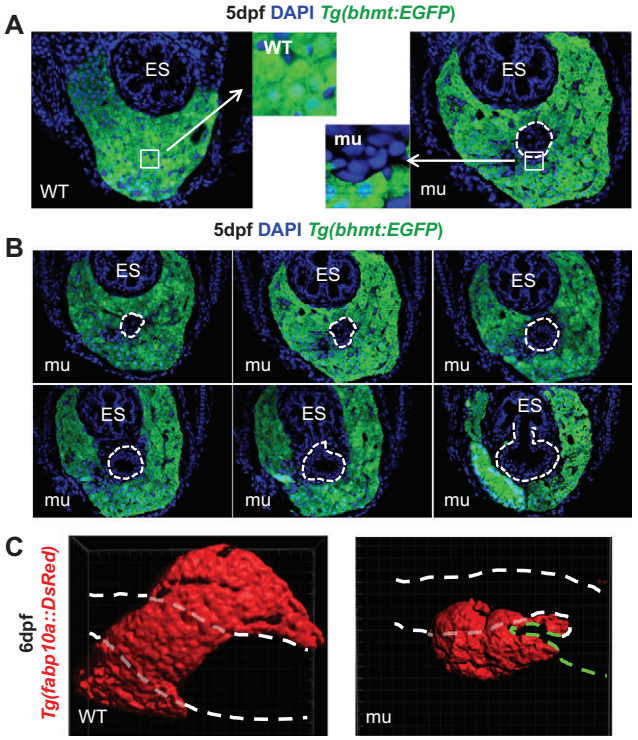

Figure 3 *hhex*^{zju1} develops an intrahepatic lumen structure. (**A**) A confocal section showing the intrahepatic lumen (circulated with a white dashed line) in the *hhex*^{zju1} mutant (mu) in the *Tg(bhmt:EGFP)* background. The insets represent the high magnification view of the boxed regions. (**B**) Consecutive confocal sections of the liver in an *hhex*^{zju1} embryo (mu) in the *Tg(bhmt:EGFP)* background showing the intrahepatic lumen (highlighted with dashed lines) is finally fused to the junction region between the esophagus (ES) and intestine. (**C**) 3D reconstruction of the liver in a WT and an *hhex*^{zju1} embryo at 6dpf, respectively, in the *Tg(fabp10a:DsRed)* background. Pair of white dashed lines, indicating the digestive tract (esophagus plus intestine); green dashed line, indicating the intrahepatic lumen structure in *hhex*^{zju1}.

hhex^{zju1} *develops an intrahepatic intestinal tube*

To further characterize the small liver phenotype in *hhex*^{zju1}, we crossed the *hhex*^{zju1} heterozygous fish (*hhex*$^{zju1/+}$) with the *Tg(bhmt:EGFP)* reporter fish to get the *Tg(bhmt:EGFP) hhex*$^{zju1/+}$ fish. Through analyzing the cryosections from the *Tg(bhmt:EGFP) hhex*^{zju1} embryos at 5dpf, we surprisingly found a lumenized structure in the mutant liver which was not present in WT (Figure 3A). By analyzing serial sections of a 5dpf-old mutant embryo, we found that this lumen structure is connected to and also opens to the main intestinal tube (Figure 3B, highlighted by dashed lines), which was never observed in a WT embryo (Supplementary Figure S2A). Besides, the cells surrounding the lumen of *hhex*^{zju1} are EGFP^{-} cells (Figure 3A and B), excluding the hepatic nature of the cells surrounding the lumen. The presence of this lumen structure in *hhex*^{zju1} is further confirmed by reconstruction of confocal images into a 3D image (Figure 3C, green dashed line). The *hhex*^{zju2} mutant also developed an intrahepatic lumen (Supplementary Figure S2B).

We went further to determine the identity of the EGFP^{-} cells surrounding the lumen. Monoclonal antibody 2F11 specifically recognizes Annexin A4 expressed in the ductal cells which can be used to mark the intrahepatic biliary ducts and the extrahepatic biliary duct part of the HPD system (Zhang et al., 2014). Immunostaining using 2F11 allowed us to clearly visualize the ductal system in the liver (Figure 4A and B: 2dpf-L, 3dpf-L, 5dpf-L, and 7dpf-L) and the gallbladder (Figure 4A and B: 5dpf-R and 7dpf-R) in WT at 3dpf, 5dpf, and 7dpf. However, in the *hhex*^{zju1} mutant, the intrahepatic biliary ducts are severely compromised (Figure 4A and B: 2dpf-L, 3dpf-L, 5dpf-L, and 7dpf-R) and the extrahepatic biliary duct part of the HPD system (including the

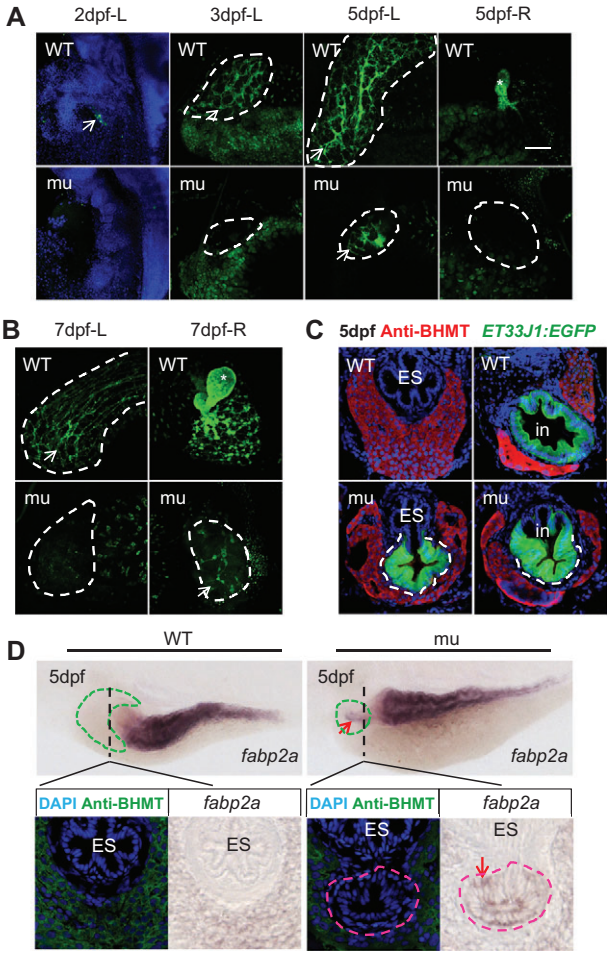

Figure 4 *hhex*^{zju1} develops an intrahepatic intestinal tube. (**A** and **B**) Immunostaining using the 2F11 antibody to compare the HPD development between the WT and *hhex*^{zju1} mutant at 2dpf, 3dpf, 5dpf and 7dpf (dpf-L: left side of the embryo; dpf-R: right side). The liver region is circulated with a white dashed line. white arrow, bile duct system; *, gallbladder. (**C**) Confocal sections of the liver in a WT and an *hhex*^{zju1} embryo (mu) in the *Tg(ET33J1:EGFP)* background showing the cells surrounding the intrahepatic lumen (highlighted with dashed lines) were EGFP-positive at 5dpf. Note that the posterior part of the esophagus (ES) was EGFP-negative in both WT and mutant. (**D**) Upper panels: WISH using the intestinal marker *fabp2a* on the WT and *hhex*^{zju1} mutant (mu) embryos at 5dpf. The liver is circulated with a green dashed line. A red arrow points to the intrahepatic lumen that is *fabp2a*-positive. Lower panels: After WISH using the *fabp2a* probe, embryos were sectioned through the plane as indicated by the black dashed line and stained with the Bhmt antibody. The intrahepatic lumen in *hhex*^{zju1} is of the nature of *fabp2a*-positive cells. DAPI: nuclei staining.

gallbladder) are not formed (Figure 4A and B: 5dpf-R and 7dpf-R). This result suggests that the lumen structure is not an outcome of over-expansion of the ductal system.

The zebrafish enhancer trapping line *Tg(ET33J1:EGFP)* (http://plover.imcb.a-star.edu.sg/webpages/ET33-J1.html) strongly expresses the reporter EGFP in the gut epithelia together with weak expression in the anterior part of the esophagus (Supplementary Figure S3). We crossed *hhex*$^{zju1/+}$ with the *Tg(ET33J1:EGFP)* and analyzed the EGFP signal in the *hhex*^{zju1} background. As expected, in the WT embryo at 5dpf, the EGFP signal was strongly expressed in the intestinal bulb, but was not observed in the liver and the posterior part of the esophagus connecting to the intestinal bulb (Figure 4C, upper panels). Interestingly, in *hhex*^{zju1}, the intrahepatic lumen displayed a strong EGFP signal that finally fused with the digestive tract at the junction between the esophagus (which is EGFP^{-}) and the intestinal bulb (Figure 4C, lower panels).

The expression of *fabp2a* is normally restricted in the intestine. Although the expression pattern of *fabp2a* in *hhex*^{zju1} appears to be similar to that in WT at 3dpf (Figure 1D), careful examination of the *fabp2a* stained 5dpf-old *hhex*^{zju1} embryos revealed that there is a short protrusion of *fabp2a*-positive cells (Figure 4D, upper panels), which looks to match the position of the lumenized structure revealed by 3D reconstruction (Figure 3C). We then sectioned the *fabp2a*-WISH embryos and found that the cells forming the lumenized structure in the *hhex*^{zju1} mutant liver were indeed of being *fabp2a*-positive (Figure 4D, lower panels). Therefore, the lumenized structure is an intrahepatic intestinalized tube.

The intrahepatic intestine is not originated from Fabp10a- or TP1-positive cells

In the transgenic fish *Tg(fabp10a:CreERT2)*, the expression of *CreERT2* is driven by the hepatocyte specific promoter *fabp10a*. Introducing *Tg(fabp10a:CreERT2)* to the *Tg(β-actin:loxP-DsRed-STOP-loxP-GFP)* background will, upon the tamoxifen treatment, genetically label all embryonic hepatocytes to express EGFP permanently (Gao et al., 2018). We first crossed *hhex*$^{zju1/+}$ with *Tg(β-actin:loxP-DsRed-STOP-loxP-GFP)* and *Tg(fabp10a:CreERT2)*, respectively, and then crossed *hhex*$^{zju1/+}$ *Tg(fabp10a:CreERT2)* fish with *hhex*$^{zju1/+}$ *Tg(β-actin:loxP-DsRed-STOP-loxP-GFP)* fish. As expected, all hepatocytes were labeled by EGFP (EGFP^{+}) in either *Tg(fabp10a:CreERT2; β-actin:loxP-DsRed-STOP-loxP-GFP)* (WT background) or *hhex*^{zju1} *Tg(fabp10a:CreERT2; β-actin:loxP-DsRed-STOP-loxP-GFP)* (mutant background) 5dpf-old embryos after the tamoxifen treatment at 36hpf (Figure 5A). Examining the liver in the 5dpf-old *hhex*^{zju1} *Tg(fabp10a:CreERT2; β-actin:loxP-DsRed-STOP-loxP-GFP)* embryos after the tamoxifen treatment at 36hpf, we found that the cells forming the intrahepatic intestinal tube in *hhex*^{zju1} were EGFP-negative cells (Figure 5A, right image panels).

In *Tg(TP1:CreERT2)*, the *Cre-ERT2* is expressed in the bile duct epithelia cells which can be adopted to trace the bile duct cell lineage (He et al., 2014) (Figure 5B, left panels). We crossed *hhex*$^{zju1/+}$ with *Tg(β-actin:loxP-DsRed-STOP-loxP-GFP)* and *Tg(TP1:CreERT2)*, respectively. We then crossed *hhex*$^{zju1/+}$ *Tg(TP1:CreERT2)* fish with *hhex*$^{zju1/+}$ *Tg(β-actin:loxP-DsRed-STOP-loxP-GFP)* fish. Treating the progenies derived from *hhex*$^{zju1/+}$ *Tg(Tp1:CreERT2; β-actin:loxP-DsRed-STOP-loxP-GFP)* with tamoxifen permanently labeled the bile duct cells as EGFP^{+} (Figure 5B). We failed to identify any EGFP^{+} cells within the intrahepatic intestinal

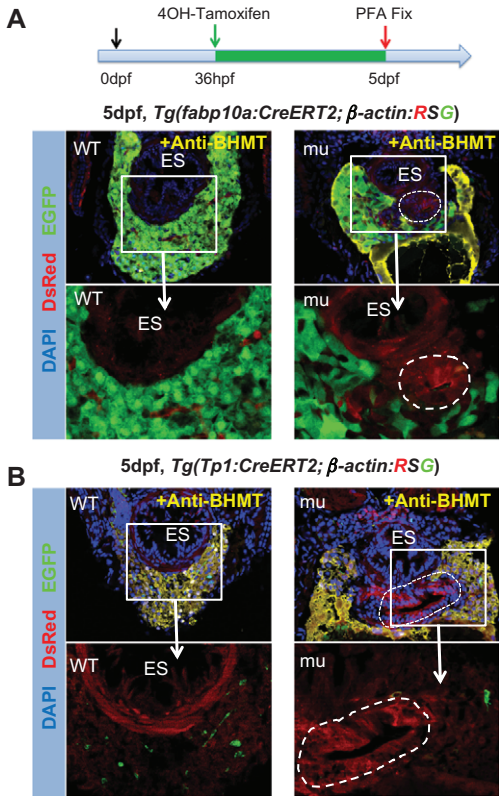

Figure 5 The intrahepatic intestinal tube is not originated from Fabp10a- or TP1-positive cells. (**A** and **B**) Upper panels: Co-immunostaining of Bhmt (yellow), DsRed (red), and EGFP (green) to examine the liver in the 5dpf-old WT and *hhex*^{zju1} (mu) embryos in the background of *Tg(fabp10a:CreERT2; β-actin:loxP-DsRed-STOP-loxP-GFP)* (for labeling hepatocytes) (**A**) or of *Tg(Tp1:CreERT2; β-actin:loxP-DsRed-STOP-loxP-GFP)* (for labeling bile duct cells) (**B**) after the tamoxifen treatment at 36hpf. Lower panels: The high magnification views of the boxed regions show that the cells forming the intrahepatic intestinal tube (circulated with a white dashed line) were EGFP-negative. DAPI was used to stain the nuclei. ES, esophagus.

tube in *hhex*^{zju1} at 5dpf after tamoxifen treatment at 36hpf (Figure 5B, right panels). Therefore, the cells surrounding the intrahepatic intestinal tube are originated neither from the differentiated hepatocytes nor form the bile duct cells.

cdx1b and pdx1 are expressed ectopically in the intrahepatic intestine in hhex^{zju1}

We asked how the intrahepatic intestinal tube is formed in *hhex*^{zju1}. The zebrafish *cdx1b* gene is a specific marker for the foregut region and is essential for the normal development of the digestive tract in zebrafish (Cheng et al., 2008). With the reference to the somite, WISH using the *cdx1b* probe showed that there is an obvious protrusion of the *cdx1b*-positive domain at the tip of the foregut in *hhex*^{zju1} at 2dpf, 3dpf, 4dpf, and 5dpf (Figure 6A, upper panels; Supplementary Figure S4A). *pdx1* is a transcription factor necessary for intestinal tube differentiation and pancreatic development in zebrafish (Yee et al., 2001). At

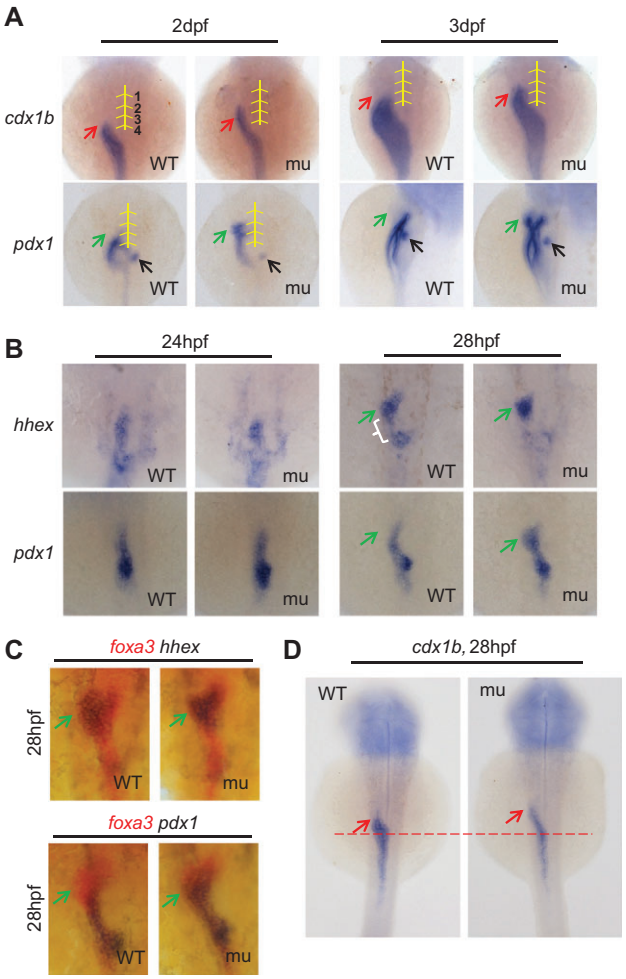

Figure 6 Loss-of-function of Hhex causes an ectopic expression of *cdx1b* and *pdx1* in the prospective hepatobiliary duct region of the HPD system at 28hpf. (**A**–**D**) WISH using the *cdx1b* or *pdx1* probe (**A**), *hhex* or *pdx1* probe (**B**), *foxa3* and *hhex* or *foxa3* and *pdx1* double probes (**C**) or *cdx1b* probe (**D**) on WT and *hhex*^{zju1} mutant (mu) embryos at different stages as shown. (**A**) An ectopic expression of *cdx1b* and *pdx1* was detected in *hhex*^{zju1} mutant (mu) embryos at 2dpf and 3dpf as shown (the middle line and somite 1–4 were indicated with yellow lines). (**B** and **C**) Ectopically expressed *pdx1* was found obviously in the cells presumably expressing *hhex* in the mutant at 28hpf. (**D**) The *cdx1b* expansion domain is extended anteriorly in the mutant at 28hpf. Bracket, prospective HPD; green arrow, liver; red arrow, the anterior edge of the intestinal bulb; horizontal red dashed line, left bending point for the endoderm rod.

2dpf and 3dpf, *pdx1* is expressed in the domains of the posterior part of the esophagus, anterior part of the intestinal tube and pancreatic duct/bud in WT (Figure 6A, lower panels). In contrast, in *hhex*^{zju1}, while the *pdx1*-positive domains in the intestinal tube and islet appeared not to be affected the domain for pancreatic bud/duct is missing at 2dpf (Figure 6A, lower panels), which nicely explains the pancreatic phenotype in *hhex*^{zju1}. Strikingly, a new *pdx1*-positive domain is formed on the left side of the intestinal tube in *hhex*^{zju1} and this domain

apparently extended into the liver region (Figure 6A, lower panels). We then performed WISH using *cdx1b* and *pdx1* double probes on embryos at 2dpf, 3dpf, and 4dpf. The result showed that the *cdx1b* signal overlapped with the *pdx1* signal along the extra domain of the digestive tract in *hhex*^{zju1} (Supplementary Figure S4B, green arrow).

In addition to its expression in the liver and pancreatic buds, *hhex* is also clearly expressed in the prospective HPD cells at 28hpf (Figure 1A). Comparing the expression patterns of *hhex* and *pdx1* showed that, seemingly, there was a significant co-expression of *hhex* and *pdx1* along the endoderm rod in WT at 24hpf (Figure 6B, left panels). However, except the islet and cells prospective for the pancreatic bud, the posterior *hhex*-positive domain started to separate from the *pdx1*-positve domain in WT by 28hpf (Figure 6B, right panels). A close look at the expression patterns of *hhex* and *pdx1* in WT at 34hpf and 40hpf showed that these two genes are clearly co-expressed in the islet and cells prospective for the pancreatic duct but not in the liver bud. It appears that *hhex* and *pdx1* are co-expressed in a few cells prospective for the hepatic duct, however, we cannot exclude the possibility that *hhex*-positive cells and *pdx1*-positive cells represent different but adjacent cells in this region (Figure 7). WISH using *hhex* and *pdx1* double probes clearly revealed that *pdx1* and *hhex* were seemingly not co-expressed in the liver bud region but were clearly co-expressed in the islet and also in the cells prospective for pancreatic duct in WT at 2dpf (Supplementary Figure S4C).

We then examined the expression patterns of *hhex*, *pdx1*, and *cdx1b* in the *hhex*^{zju1} mutant further. WISH using the *hhex* probe showed that the *hhex*^{zju1} mutant produced *hhex* transcripts in the liver bud (Figure 6B, upper panels), suggesting that the transcription of *hhex* in the liver bud is not affected by the *hhex*^{zju1} mutation. However, the *hhex* transcripts were almost abolished in the region prospected for the exocrine pancreas in the *hhex*^{zju1}

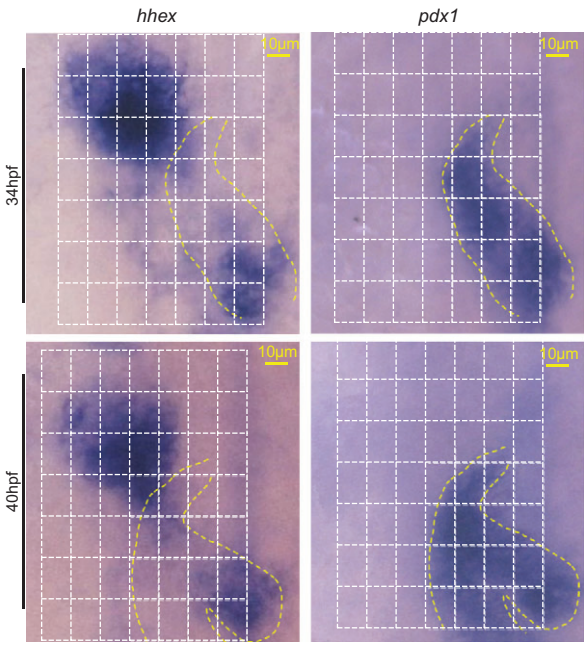

Figure 7 Comparison of expression patterns of *hhex* and *pdx1*. WISH using an *hhex* or *pdx1* probe was performed on WT embryos at 34hpf and 40hpf. Images were gridded with white dashed lines (the first vertical line on the right was aligned with the middle line of the embryo) to facilitate the comparison. *pdx1*-positive cells and their corresponding region in *hhex* WISH are circulated with a yellow dashed line.

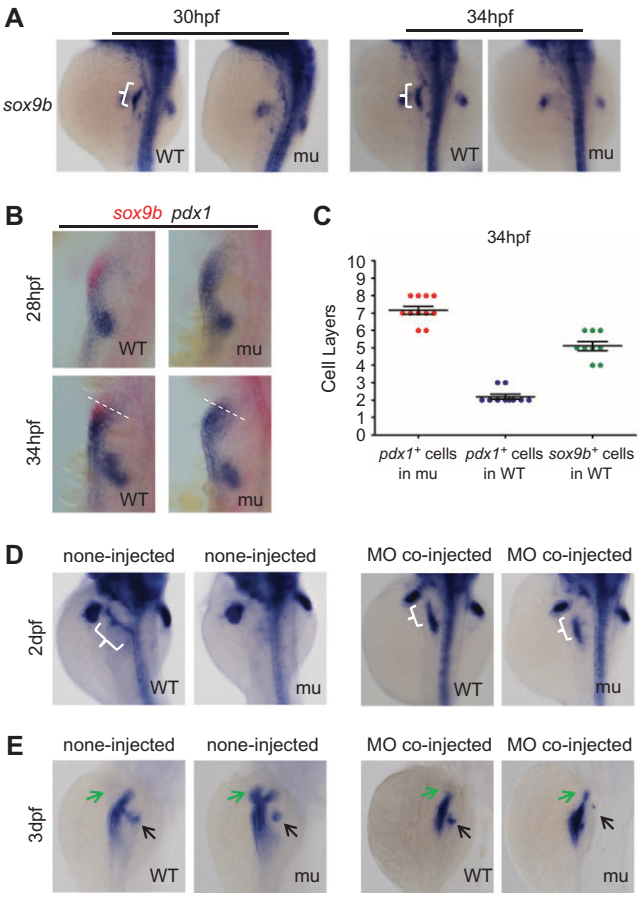

Figure 8 Loss-of-function of Hhex abolishes the sox9b expression and co-injection of *cdx1b* and *pdx1* specific morpholinos restores the *sox9b* expression. (**A**) WISH using *sox9b* probe on WT and *hhex*^{zju1} mutant (mu) embryos at 30 hpf and 34 hpf. *sox9b* transcripts were undetectable in the HPD area but were clearly visible in other regions including the fin bud in the mutant. (**B**) WISH using the *sox9b* and *pdx1* double probes on WT and *hhex*^{zju1} (mu) embryos at 28 hpf and 34 hpf. Notice that the ectopic *pdx1*-positive cells in *hhex*^{zju1} corresponded to the *sox9b*-positive cells in WT. (**C**) Statistical data of layers of *sox9b* (*sox9b*$^{+}$) and *pdx1* (*pdx1*$^{+}$) positive cells calculated along the dashed white line in **B** in WT and *hhex*^{zju1} embryos at 34hpf. (**D**) Co-injection of *cdx1b* and *pdx1* specific morpholinos restored the *sox9b* expression in the mutant HPD at 2dpf. (**E**) Co-injection of *cdx1b* and *pdx1* specific morpholinos resulted in the disappearance of *pdx1* ectopic expression in the mutant HPD. White bracket, prospective HPD; green arrow, liver; black arrow, pancreatic bud.

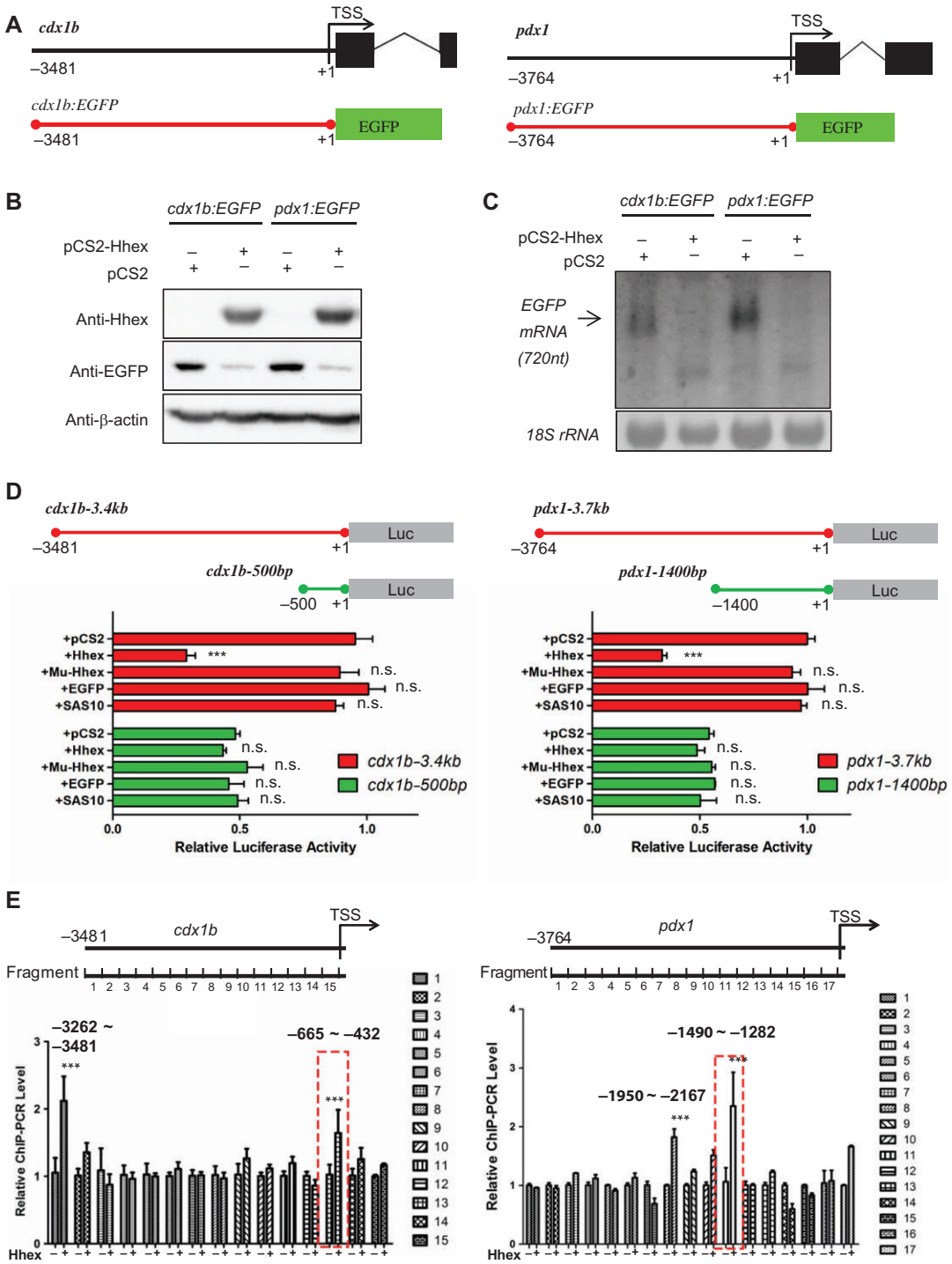

Figure 9 Hhex represses the transcriptional activity of *cdx1b* and *pdx1* promoters. (**A**) Diagram showing the promoter fragment of *cdx1b* (3481 bp, left panel) and *pdx1* (3764 bp, right panel) and their corresponding reporter construct *cdx1b:EGFP* and *pdx1:EGFP*. TSS, translation start site. (**B** and **C**) Western blotting of EGFP protein (**B**) and northern blotting of the *egfp* transcripts (**C**) in the *cdx1b:EGFP* or *pdx1:EGFP* plasmid-transfected HCT116 cells with or without the pCS2-Hhex plasmid. (**D**) The *cdx1b* promoter regions –1 to –3481 bp (*cdx1b-3.4kb*) and –1 to –500 bp (*cdx1b-500bp*) (left panels) and the *pdx1* promoter regions –1 to –3764 bp (*pdx1-3.7kb*) and –1 to –1400 bp (*pdx1-1400bp*) (right panels) were cloned to the pGL3 vector, respectively. Luciferase activity assays showed that Hhex, but not EGFP, SAS10, or Hhex^{zju1} mutant protein (Mu-Hhex), repressed the transcriptional activity of the *cdx1b-3.4kb* and *pdx1-3.7kb* but not of the *cdx1b-500bp* and *pdx1-1400bp*. (**E**) ChIP-PCR screening of the *cdx1b* and *pdx1* promoters. The *cdx1b-3.4kb:luc* or *pdx1-3.7kb:luc* plasmid was co-transfected with or without Hhex-expressing plasmid (*pCS2-HA-Hhex*) into the HCT116 cells. Protein samples from such cells were subjected to ChIP assay

mutant at 28hpf (Figure 6B, upper panels). We observed that there was an ectopic expression of *pdx1* in the prospective liver bud area at 28hpf (Figure 6B, lower panels) and 2dpf (Supplementary Figure S4C) but did not observe obvious difference at 24hpf in *hhex*^{zju1} (Figure 6B, lower panels). *foxa3* is a pan-endoderm marker. Comparing the signal patterns between WISH using the *foxa3* and *hhex* double probes and *foxa3* and *pdx1* double probes revealed that *pdx1* was expressed ectopically in the cells presumably expressing *hhex* in the *hhex*^{zju1} mutant (Figure 6C). WISH using *hhex* and *cdx1b* double probes showed that these two genes were expressed in distinctive regions in WT at 2dpf (Supplementary Figure S4D). However, WISH using the *cdx1b* probe showed that there is a protrusion of the *cdx1b*-positive domain at the tip of the foregut in *hhex*^{zju1} at 28hpf (Figure 6D). In WISH embryos using *cdx1b* and *hhex* double probes, we identified a great proportion of *hhex*-positive cells (expressing the *hhex*^{zju1} mutant transcript) also expressing *cdx1b* at 2dpf (Supplementary Figure S4D). These results suggest that the ectopic expression of *pdx1* and *cdx1b* in the *hhex*-positive cells in the *hhex*^{zju1} mutant happens at the early stage of organogenesis of the digestive system.

Intrahepatic intestine in hhex^{zju1} *is formed at the expense of the HPD system*

The transcription factor gene *sox9b* has recently been identified to be a specific marker and also an essential gene for the development of the HPD system (Delous et al., 2012; Manfroid et al., 2012). We performed a WISH using the *sox9b* probe. As expected, *sox9b* is expressed in the HPD cells at 30hpf, 34hpf (Figure 8A), 38hpf, 40hpf, 48hpf, and 72hpf (Supplementary Figure S5). However, the *sox9b* transcripts were undetectable in the prospected HPD cells in the *hhex*^{zju1} mutant at these time points (Figure 8A; Supplementary Figure S5), demonstrating that the *hhex*^{zju1} mutant fails to develop the HPD system. We asked whether the ectopic expression of *cdx1b* and *pdx1* in the extra domain in the *hhex*^{zju1} mutant was at the expense of the HPD cells. To verify this hypothesis, we compared the expression patterns of *sox9b* and *pdx1* with reference to the expression patterns of *hhex* in WT and *hhex*^{zju1} (expressing *hhex*^{zju1} mutant transcript). We found that, at 34hpf, 40hpf, and 48hpf, the ectopically expressed *pdx1* in the *hhex*^{zju1} mutant clearly corresponded to the region prospected for *sox9b*-positive cells in WT (Supplementary Figures S6–S8). We then performed a WISH using *sox9b* and *pdx1* double probes (Figure 8B). The results based on calculating the cell layers with reference to the middle line showed that the *sox9b*-positive domain was seemingly completely replaced by *pdx1*-positive cells in the *hhex*^{zju1} mutant (Figure 8C).

Next, we co-injected *cdx1b* and *pdx1* specific morpholinos into the WT and *hhex*^{zju1} embryos to knock down the expression of these two genes. We observed that the expression of *sox9b* was restored in *hhex*^{zju1} at 48hpf (Figure 8D). Furthermore, WISH using *pdx1* showed that co-injection of *cdx1b* and *pdx1* morpholinos eliminated the ectopically expressed *pdx1* in *hhex*^{zju1} at 3dpf (Figure 8E). However, the expression of *Annexin A4*, the biliary marker, was not restored in the morphants, suggesting that the HPD cell fate was not fully restored (Supplementary Figure S9A). On the other hand, injection of *cdx1b* or *pdx1* single morpholinos failed to restore the *sox9b* expression (Supplementary Figure S9B) in the *hhex*^{zju1} mutant. These results suggest that loss-of-function of *hhex* abolishes the expression of *sox9b* and leads to the ectopic expression of *pdx1* and *cdx1b* in the HPD cells prospective for the extrahepatic biliary duct that finally developed into an intrahepatic intestine tube. Therefore, we hypothesize that Hhex determines the extrahepatic biliary duct cells fate by repressing the expression of *cdx1b* and *pdx1*.

Hhex represses the expression of cdx1b and pdx1 to safeguard the development of the HPD system

The lack of the *sox9b*-positive cells in *hhex*^{zju1} suggests that Hhex is essential for the differentiation of the HPD cells. Previous studies have shown that Hhex acts either as an activator or a repressor to regulate the expression of its downstream genes (Soufi and Jayaraman, 2008). The ectopic expression of *cdx1b*- and *pdx1*-positive cells in *hhex*^{zju1} suggests that Hhex might negatively regulate the expression of these two genes so that to prevent the differentiation of the extrahepatic biliary part of the HPD cells to gut epithelia. To determine the relationship between Hhex and *cdx1b* or *pdx1* expression, we obtained a 3481-bp and a 3764-bp genomic DNA fragment upstream of the translation start site ATG of *cdx1b* and *pdx1*, and cloned them to the upstream of the *EGFP* reporter gene to get *cdx1b:EGFP* and *pdx1:EGFP*, respectively (Figure 9A). The *cdx1b:EGFP* and *pdx1:EGFP* plasmids were used to transfect HCT116 (Human colorectal carcinoma) cells that are known to express human *cdx2* and *pdx1* (https://www.ebi.ac.uk/gxa/experiments/E-MTAB-2706/Results), respectively. Examination of the EGFP fluorescence (Supplementary Figure S10A and B) and western blot analysis of the EGFP protein (Figure 9B) showed that both plasmids achieved the expression of the *EGFP* gene, suggesting that the DNA fragments cloned harbored the promoter activity for the expression of *cdx1b* and *pdx1*, respectively.

We co-transfected the *pCS2-CMV:hhex* plasmid with either *cdx1b:EGFP* or *pdx1:EGFP*. Hhex was robustly expressed in the transfected HCT116 cells (Figure 9B). Analyzing EGFP-fluorescence and -protein showed that, compared to the cells transfected with the *pCS2*-vector plus *cdx1b:EGFP* or *pCS2*-vector plus *pdx1:EGFP*, expression of Hhex suppressed the expression of EGFP (Figure 9B; Supplementary Figure S10) by transcriptionally downregulating

using an antibody against the HA-tag. Fifteen (for *cdx1b-3.4kb*) and 17 (for *pdx1-3.7kb*) pairs of specific primers were designed, respectively, to amplify 15 and 17 DNA fragments covering the entire promoter sequences of *cdx1b* 3481 bp (left panels) and *pdx1* 3764 bp (right panels), respectively. All luciferase activity was normalized with Renilla luciferase vectors (phRL-TK) as the reference. $^{**}P < 0.01$; $^{***}P < 0.001$; n.s., no significance.

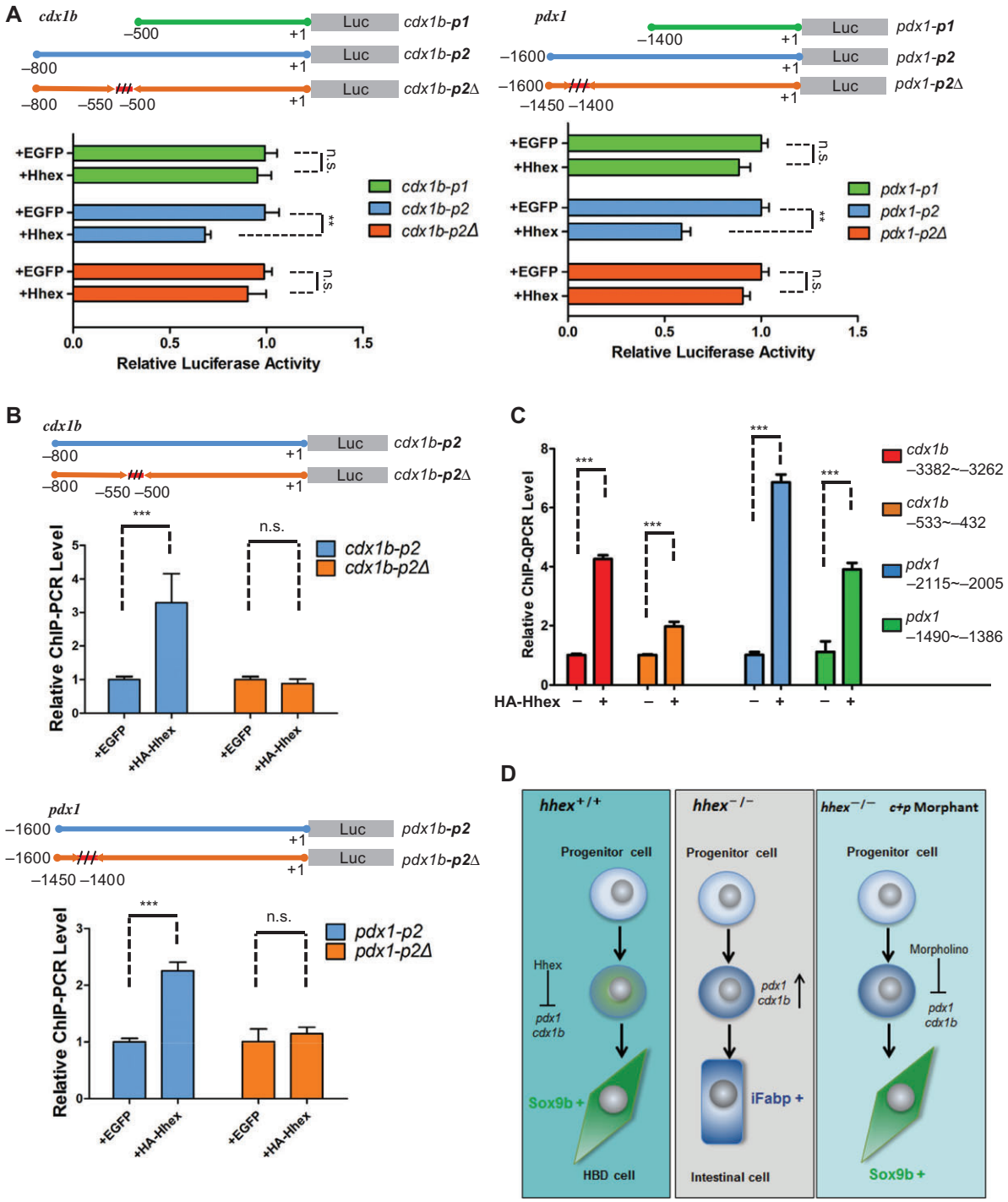

Figure 10 Hhex binds to the endogenous promoters of *cdx1b* and *pdx1*. (**A**) Three *cdx1b* promoter reporter plasmids, *cdx1b-p1* (–1 to –500 bp), *cdx1b-p2* (–1 to –800 bp), and *cdx1b-p2Δ* (deleted –500 to –550 bp region in *cdx1b-p2*) (left panels), and three *pdx1* promoter reporter plasmids, namely *pdx1-p1* (–1 to –1400 bp), *pdx1-p2* (–1 to –1600 bp), and *pdx1-p2Δ* (deleted –1400 to –1450 region in *pdx1-p2*) (right panels), were constructed. Luciferase activity assays show that the sequences between –500 and –550 bp in *cdx1b-p2* and –1400 to –1450 bp in *pdx1-p2* contain the Hhex-responsive elements. (**B**) qPCR analysis of the ChIP products revealed that the internal deletion of –500 to –550 bp in *cdx1b-p2* (*cdx1b-800bp*) (upper panels) and of –1400 to –1450 bp in *pdx1-p2* (*pdx1-1600bp*) (lower panels) abolished the enrichment of *cdx1b-p2Δ* and *pdx1-p2Δ* by Hhex. (**C**) ChIP-PCR analysis of Hhex binding to the endogenous promoters of *cdx1b* and *pdx1* in the embryos co-injected with *hhex* and *cas* mRNA. Primer pairs for qPCR covering the specific *cdx1b* or *pdx1* regions were shown. All luciferase activity was normalized with Renilla luciferase vectors (phRL-TK) as the reference. $^{**}P < 0.01$; $^{***}P < 0.001$; n.s., no significance. (**D**) A model to depict the genetic network controlling the patterning and organogenesis of the HPD system. Based on the expression patterns of *hhex*, *cdx1b*, and *pdx1* in WT and

the expression of *EGFP* (Figure 9C). To better quantify the effect of Hhex on the promoter activity of *cdx1b* and *pdx1*, we cloned the reporter gene *Firefly luciferase* (*luc*) downstream of the *cdx1b* (*cdx1-3.4kb:luc*) and *pdx1* (*pdx1-3.7kb:luc*) promoter, respectively (Figure 9D, upper panels). Co-transfection analysis showed that Hhex, but not EGFP, Sas10 (a nucleolar protein) (Wang et al., 2016), or Hhex^{zju1} mutant protein, strongly suppressed the expression of Luc in *cdx1b-3.4kb:luc* and *pdx1-3.7kb:luc* (Figure 9D, lower panels).

Hhex is reported to bind to a consensus sequence 5′-YWATTAAR-3′ (Crompton et al., 1992). By searching the promoter sequences, we identified four and five putative Hhex-binding consensus sequences in the promoters for *cdx1b* and *pdx1*, respectively (Supplementary Figure S11A). However, deleting all four motifs in *cdx1b* (*cdx1b-ΔHRE1-4*) or all five motifs in *pdx1* (*pdx1-ΔHRE1-5*) did not alter the repressive effect of Hhex on the *pdx1* and *cdx1b* promoters (Supplementary Figure S11B). To determine the Hhex-responsive elements in the *pdx1* and *cdx1b* promoters, we performed ChIP using protein samples extracted from the *pCS2-HA-Hhex* plus *pdx1:luc* or *pCS2-HA-Hhex* plus *cdx1b:luc* co-transfected HCT116 cells. ChIP products were analyzed by qPCR using specific primers (Supplementary Table S2) covering every 200 bp of the *pdx1* 3764-bp and *cdx1b* 3481-bp DNA fragment (Figure 9E, upper panels). Two regions in *cdx1b* promoter (−432 to −665 and −3262 to −3481) and two regions in *pdx1* promoter (−1282 to −1490 and −1950 to −2167) were identified to be enriched by the HA-tag antibody (Figure 9E, lower panels).

We then generated a series of promoter deletion constructs and found that the −1 to −500 bp region in *cdx1b* and the −1 to −1400 bp region in *pdx1* have lost responses to the repressive effect of Hhex on the *luc* expression (Supplementary Figure S11C), suggesting that these regions do not harbor the Hhex-responsive elements. On the other hand, the −1 to −600 bp or to −800 bp of *cdx1b* and −1 to −1500 bp or to −1600 bp of *pdx1* exhibited strong response to the repressive effect of Hhex on the *luc* expression (Supplementary Figure S11C), which is consistent with the ChIP analysis (Figure 9E). We therefore focused on the −1 to −600 bp region in *cdx1b (cdx1b-p2)* and −1 to −1500 bp region in *pdx1 (pdx1-p2)*. We generated different internal deletion constructs and found that deleting the −500 to −550 bp region in *cdx1b-p2* and the −1400 to −1450 bp region in *pdx1-p2* lost responsiveness to the repressive effect of Hhex on the luciferase activity (Figure 10A). ChIP-PCR analysis showed that, compared to *cdx1b-p2* and *pdx1-p2*, Hhex is indeed no longer enriched in *cdx1b-p2Δ* or *pdx1-p2Δ* (Figure 10B).

To determine whether Hhex binds to the endogenous promoters of *cdx1b* and *pdx1*, we injected *hhex* (fused with an HA-tag) mRNA together with *casanova* (*cas*) mRNA into the WT embryos at one-cell stage. Cas is a master determinant of endoderm cell fate during early embryogenesis (Kikuchi et al., 2001). As expected, WISH using the endoderm marker *sox17* (Kikuchi et al., 2001) showed that, compared to a normal WT, nearly all cells in the *cas* mRNA injected embryos at 8hpf became *sox17*-positive (Supplementary Figure S12A). Western blot analysis showed that Hhex was robustly expressed in the *hhex* mRNA injected embryos at 6hpf (Supplementary Figure S12B). Total protein was respectively extracted from *cas* mRNA alone injected embryos and *hhex* plus *cas* mRNA co-injected embryos and was subjected to ChIP-PCR analysis. ChIP-PCR was performed on the sites identified by promoter screening in the luciferase activity assay for *cdx1b* and *pdx1*, respectively (Figure 9E). We found that Hhex was significantly enriched in the −3262 to −3382 (~4-fold enrichment) and −432 to −533 (~2-fold enrichment) regions in the promoter of *cdx1b* when using exon 3 of *cdx1b* as a reference (Figure 10C). Similarly, Hhex was significantly enriched in the −2005 to −2115 (~7-fold enrichment) and −1386 to −1490 (~4-fold enrichment) regions in the promoter of *pdx1* when using exon 2 of *pdx1* as a reference (Figure 10C).

Discussion

In zebrafish, *hhex* is expressed in the foregut endoderm region at 26hpf (Ober et al., 2006), and then extended to the liver, pancreas and HPD cells (Huang et al., 2008). Importantly, we show here that zebrafish *hhex*-null mutant can survive up to 7dpf. Considering the fact that zebrafish digestive organs are clearly identifiable by 52hpf, the *hhex* null mutant provides an ideal model to study the role of Hhex not only in the liver and pancreas development but also in the HPD development.

We show here that the zebrafish *hhex* null mutant *hhex*^{zju1} develops a small liver, suggesting that Hhex is not necessary for liver specification but is essential for liver bud growth as that observed in mice (Bort et al., 2004). The *hhex*^{zju1} mutant fails to develop a detectable exocrine pancreas, which coincides with its role in the development of ventral pancreas in mouse (Bort et al., 2004). The *hhex*^{zju1} mutant also lacks the HPD system as that reported in mice (Bort et al., 2006; Hunter et al., 2007). In contrast, loss-of-function of Hhex does not affect the overall development of the intestine. Therefore, Hhex is a key factor controlling the organogenesis of the auxiliary digestive organs including liver, pancreas and the HPD system but not the main digestive tract, nicely coinciding with its dynamic expression patterns.

Anatomic analysis revealed that *hhex*^{zju1} develops an intrahepatic lumen that is fused to the main intestinal tract. Cell lineage tracing study showed that this intrahepatic lumen is not

hhex^{zju1}, together with the analysis of the effect of Hhex on the promoters of *cdx1b* and *pdx1* genes, we propose that, in the WT HPD precursor cells, Hhex suppresses the expression of *cdx1b* and *pdx1* to safeguard the hepatobiliary duct cell fate in the HPD system. In *hhex*^{zju1}, due to the absence of Hhex, the hepatobiliary duct precursor cells express Cdx1b and Pdx1 that changes the HPD cell fate to the intestinal epithelial cell fate that finally leads to the formation of an intrahepatic intestinal tube in *hhex*^{zju1}. Morpholino-mediated knockdown of *cdx1b* and *pdx1* restores the *sox9b* expression in the HPD in *hhex*^{zju1}. It appears that Cdx1b or Pdx1 or together, directly or indirectly suppresses the *sox9b* expression.

originated from the hepatocytes or bile duct cells. Analysis of the expression of the intestinal marker *fabp2a* revealed that the cells forming the intrahepatic lumen were the nature of intestinal epithelia. Therefore, *hhex*^{zju1} develops an intrahepatic intestinal tube. This phenotype can be explained by the fact that *cdx1b* and *pdx1*, two genes essential for the digestive tract organogenesis, are expressed not only in the normal intestinal epithelium but also ectopically in the intrahepatic lumen in *hhex*^{zju1}.

Considering the fact that *sox9b* signal was not detected in the prospected HPD region in the *hhex*^{zju1} mutant, it is reasonable to speculate that the intrahepatic intestinal tube is originated from the HPD precursor cells. There are four lines of evidences to support this hypothesis. Firstly, it has been shown that the Hhex progenitors conferred a duodenal fate in the *Hhex*-null mice (Bort et al., 2006). In addition, the extrahepatic biliary duct is almost replaced by duodenum in the mice with conditional knockout of Hhex in the early endoderm cells (Hunter et al., 2007). Therefore, it appears that, by default, the endoderm lacking Hhex is destined to the duodenal fate. Secondly, WISH revealed that most of the *hhex*-expression domain becomes *pdx1*-positive at 28hpf in the *hhex*^{zju1} mutant. Our data are consistent with the previously reported relationship between the expression patterns of *hhex* and *pdx1* (Chung et al., 2008; Xu et al., 2016). Thirdly, we show that Hhex directly repress the promoter activities of *cdx1b* and *pdx1* genes. Therefore, it is reasonable to propose that the expanded population of *pdx1*-positive cells yields the intrahepatic intestinal tube in the *hhex*^{zju1} mutant. Finally, we found that knockdown of *cdx1b* and *pdx1* restored the expression pattern of *sox9b* in the prospected HPD domain in the *hhex*^{zju1} mutant, further confirming the fate conversion of the HPD cells to the intestinal epithelial cells. These data also suggest that the *sox9b* gene is not a direct target of Hhex. Considering the fact that *hhex*^{zju1} confers a small liver phenotype it is reasonable to speculate that the intrahepatic intestinal tube develops *in situ* rather than due to outgrowth of the liver to cover the prospected HPD.

Based on the above, we propose a genetic network that orchestrates the organogenesis of the auxiliary digestive organs including liver, exocrine pancreas, and the HPD system. Hhex is expressed in the liver and pancreas buds and in the HPD precursor cells. The fact that loss-of-function of Hhex affects the development of these organs suggests that Hhex functions as a positive regulator controlling the organogenesis of these organs. Sox9b is expressed in the HPD precursor cells in WT (Delous et al., 2012; Manfroid et al., 2012), however, the expression of *sox9b* is absent in the HPD precursor cells in *hhex*^{zju1}, suggesting that Hhex genetically acts upstream of Sox9b although the exact relationship between Hhex and Sox9b remain to be elucidated. In a WT embryo, Cdx1b is expressed in the foregut region of the endoderm while Pdx1 is expressed not only in the foregut region but also in pancreatic duct precursors. However, these two genes are absent in the extra-hepatobiliary duct precursor cells (Field et al., 2003a; Cheng et al., 2008). Hhex suppresses the expression of *cdx1b* and *pdx1* in the WT hepatobiliary duct precursor cells so that to safeguard the HPD cell fate in the hepatobiliary duct region. In *hhex*^{zju1}, due to the absence of Hhex, the HPD precursor cells prospective for hepatobiliary duct ectopically express Cdx1b and Pdx1 that changed the HPD cell fate to the intestinal epithelial cell fate that finally leads to form the intrahepatic intestinal tube in *hhex*^{zju1} (Figure 10D). In contrast, it appears Hhex has a positive role in regulating the expression of *pdx1* in the pancreatic duct of the HPD system since *pdx1* signal is almost undetectable in the pancreatic duct in *hhex*^{zju1}, leaving a question to be addressed in the future. Pdx1 is a well-known factor for specifying the pancreas as well. The domain with ectopic expression of *pdx1* in *hhex*^{zju1} did not become a part of pancreas, which suggests that Pdx1 alone is not sufficient to specify a pancreatic fate or Cdx1b or an unknown factor suppresses the Pdx1's pancreatic function. Further investigation is needed to unravel the molecular mechanism behind.

Materials and methods

Ethics statement

All animal procedures were performed in full accordance to the requirement by 'Regulation for the Use of Experimental Animals in Zhejiang Province'. This work is approved by the Animal Ethics Committee in the School of Medicine, Zhejiang University (ETHICS CODE Permit No. ZJU2011-1-11-009Y).

Fish lines and maintenance

Zebrafish AB strain was used in all experiments and for generating transgenic or mutant lines. To generate zebrafish transgenic line *Tg(bhmt:EGFP)*, a 5.2-kb genomic DNA fragment upstream of the start codon ATG of the *bhmt* gene is cloned with primer pair 5′-GCCATCCATGGCCCACATTCGT-3′ (forward primer) and 5′-GTTGATCTGATTCAGGAACAGCAGAT-3′ (reverse primer). The *bhmt:EGFP* construct was generated by subcloning EGFP cassettes downstream of the promoter sequences of *bhmt*. The *bhmt:EGFP* construct was linearized by *Hin*dIII, followed by injection into zebrafish embryos at the one-cell stage. The *Tg(bhmt:EGFP)* line was identified in the F1 generation. To generate *hhex* mutant, we synthesized gRNA against the first exon of zebrafish *hhex* gene according to the protocol described previously (Chang et al., 2013). The *Cas9* mRNA and *hhex*-targeting gRNA were co-injected into the WT embryos at the one-cell stage. The *hhex* mutant lines were identified in the F1 generation by analyzing the PCR product using primer pair hhex ID (Supplementary Table S1). For Cre/loxP-mediated lineage tracing, *Tg(fabp10a:CreERT2)* or *Tg(Tp1:CreERT2)* (He et al., 2014) embryos in the background of *Tg(β-actin:loxP-DsRed-STOP-loxP-GFP)* were treated with 10 mM 4-hydroxytamoxifen (4-OHT) at 36hpf for 3.5 days.

WISH

The embryos were fixed in 4% PFA (PBS) for 12 h at 4°C. WISH probes were labeled with digoxigenin (DIG, Roche Diagnostics). Probes *prox1*, *fabp10a*, *trypsin*, *insulin*, *fabp2a*, *foxa2*, *gata6*, and *hhex* were used as described (Huang et al.,

2008). For *cdx1b*, *sox9b*, and *pdx1* probes, primers were designed based on available sequence data and PCR products were cloned into the pGEM-T Easy Vector (Promega) (Supplementary Table S1).

Cryosectioning and immunofluorescence staining

The embryos were fixed in 4% PFA (PBS) for 1 h at room temperature. After washing in PBST (0.1% Tween 20 in PBS), the tails of embryos were clipped for genomic DNA extraction for genotyping, and the rest parts were mounted with 1.5% agarose dissolved in 30% sucrose PBS and then equilibrated overnight at 4°C. The blocks were mounted with OCT compound (Sakura). The sections were cut serially to an 11-μm thickness and collected on poly-L-lysine coated glass slides (CITOGLAS, 188105). Immunofluorescence staining was performed as described (Guan et al., 2016). Rabbit polyclonal antibody against zebrafish Fabp10a (1:500) and mouse monoclonal antibody against zebrafish Bhmt (1:500) were generated by Hangzhou HuaAn Biotechnology Company. P-H3 antibody was purchased from Santa Cruz (sc-8656-R, 1:600), PCNA antibody from Sigma (P8825, 1:1000), and 2F11 monoclonal antibody from Abcam (ab71286, 1:500). Alexa Fluor 647-labeled secondary antibody was used for visualization.

RNA and protein analysis

RNA gel blot hybridization (northern blot) was performed as described (Huang et al., 2008). *EGFP* full-length probe was DIG-labeled. Western blot was performed as described (Guan et al., 2016) using a mouse monoclonal antibody against zebrafish Hhex (1:200, HuaAn Biotechnology Company), anti-β-Actin antibody (1:1000, HuaAn R1207-1), and anti-EGFP antibody (1:1000, Santa Cruz sc-9996).

Morpholino injection

cdx1b (1 pmol) and *pdx1* (1 pmol) ATG morpholino were injected alone or co-injected into one-cell stage embryos. Morpholinos sequences were designed to target *cdx1b* ATG start codon site (5′-TCTAGGAGATAACTCACGTACATTT-3′) (Flores et al., 2008) or *pdx1* ATG codon start site (5′-GATAGTAATGCTCTTCCCG ATTCAT-3′) (Kimmel et al., 2011).

Luciferase assay

A series *cdx1b* or *pdx1* promoters were cloned into the pGL3 vector with specific primer pairs (Supplementary Table S1). Dual-luciferase reporter assays were carried out in cultured HepG2 cells or HCT116 cells. Cells were seeded in 24-well tissue culture plates 24 h prior to transfection. All transfections were performed in triplicate. For each well, co-transfection was carried out using 100 ng of promoter assay plasmid (Firefly luciferase plasmids derived from pGL3), 30 ng of either an empty expression vector (pCS2) or an expression vector encoding Hhex (pCS2-Hhex), 10 ng of a control plasmid (Renilla luciferase vectors, phRL-TK) for normalizing the transfection efficiency, and 1 μl PolyJet DNA Transfection Reagent (Signagen, SL100688) at 70%–80% confluence. The cells were harvested 24 h after transfection and assayed using the Dual-Luciferase® Reporter Assay System (Promega, Cat#E1910).

ChIP-PCR

ChIP using proteins from cultured cells was performed with slight modifications of the procedure described previously (Gong et al., 2015). HCT116 or HepG2 cells were seeded in 6-cm tissue culture dishes 24 h prior to transfection. For each well, co-transfection was carried out using 500 ng of promoter assay plasmid (Firefly luciferase plasmids derived from pGL3), 200 ng of either a control expression vector encoding EGFP (pCS2-EGFP) or an expression vector encoding HA-Hhex (pCS2-HA-Hhex), 5 μl PolyJet DNA Transfection Reagent (Signagen) at 70%–80% confluence. At 24 h post transfection, formaldehyde was added directly to tissue culture medium to a final concentration of 1% for 10 min at 37°C and was then stopped by the addition of glycine to a final concentration of 0.125 M. Cells were harvested and sonicated to shear DNA to lengths ~300 base pairs. After centrifuging the samples, the supernatant was incubated overnight at 4°C with 20 μl Anti HA-tag agarose beads (Abmart, M20013L). After serious extensively washing as described, the beads carried with antibody-protein–DNA complexes were added with proteinase-K reaction mix and heated at 65°C overnight to reverse protein–DNA crosslinks. *In vivo* ChIP (using protein from fish embryos) was performed as described (Bogdanovic et al., 2013). *HA-hhex* mRNA (50 pg) and *casanova* (*cas*) mRNA(50 pg) were co-injected into one-cell stage embryos. Embryos were collected at 6 hpf and treated with 4% PFA. The bound DNA fragments were purified by phenol/chloroform extraction and ethanol precipitation, and analyzed by Real-time Quantitative PCR (qPCR) Detecting System using specific primers (Supplementary Table S2).

Statistical analysis

Statistical analyses were performed with the Student's *T*-test. $*P < 0.05$; $**P < 0.01$; $***P < 0.001$; n.s., no significant difference.

Supplementary material

Supplementary material is available at *Journal of Molecular Cell Biology* online.

Acknowledgements

The authors thank Drs Bin Zhao, Caiqiao Zhang, and Hai Song, as well as all members in Jingrong Peng and Jun Chen labs for their valuable suggestions. The authors are grateful to Yixin Ye, Xiaocai Du, and Zhengxin Xu for their technical support with animal studies.

Funding

This work was funded by the '973 Program' of the Ministry of Science and Technology of the People's Republic of China (2015CB942802 and 2017YFA0504501) and the National Natural Science Foundation of China (http://www.nsfc.gov.cn/) (31330050 and 31571495).

Conflict of interest: none declared.

References

Arterbery, A.S., and Bogue, C.W. (2016). Hhex is necessary for the hepatic differentiation of mouse ES cells and acts via Vegf signaling. PLoS One *11*, e0146806.

Bogdanovic, O., Fernandez-Minan, A., Tena, J.J., et al. (2013). The developmental epigenomics toolbox: ChIP-seq and MethylCap-seq profiling of early zebrafish embryos. Methods *62*, 207–215.

Bogue, C.W., Ganea, G.R., Sturm, E., et al. (2000). Hex expression suggests a role in the development and function of organs derived from foregut endoderm. Dev. Dyn. *219*, 84–89.

Bort, R., Martinez-Barbera, J.P., Beddington, R.S., et al. (2004). Hex homeobox gene-dependent tissue positioning is required for organogenesis of the ventral pancreas. Development *131*, 797–806.

Bort, R., Signore, M., Tremblay, K., et al. (2006). Hex homeobox gene controls the transition of the endoderm to a pseudostratified, cell emergent epithelium for liver bud development. Dev. Biol. *290*, 44–56.

Chang, N., Sun, C., Gao, L., et al. (2013). Genome editing with RNA-guided Cas9 nuclease in zebrafish embryos. Cell Res. *23*, 465–472.

Cheng, P.Y., Lin, C.C., Wu, C.S., et al. (2008). Zebrafish cdx1b regulates expression of downstream factors of Nodal signaling during early endoderm formation. Development *135*, 941–952.

Chung, W.S., Shin, C.H., and Stainier, D.Y. (2008). Bmp2 signaling regulates the hepatic versus pancreatic fate decision. Dev. Cell *15*, 738–748.

Cong, R., Jiang, X., Wilson, C.M., et al. (2006). Hhex is a direct repressor of endothelial cell-specific molecule 1 (ESM-1). Biochem. Biophys. Res. Commun. *346*, 535–545.

Crompton, M.R., Bartlett, T.J., MacGregor, A.D., et al. (1992). Identification of a novel vertebrate homeobox gene expressed in haematopoietic cells. Nucleic Acids Res. *20*, 5661–5667.

Delous, M., Yin, C., Shin, D., et al. (2012). Sox9b is a key regulator of pancreaticobiliary ductal system development. PLoS Genet. *8*, e1002754.

Denson, L.A., McClure, M.H., Bogue, C.W., et al. (2000). HNF3β and GATA-4 transactivate the liver-enriched homeobox gene, Hex. Gene *246*, 311–320.

Dong, P.D., Munson, C.A., Norton, W., et al. (2007). Fgf10 regulates hepatopancreatic ductal system patterning and differentiation. Nat. Genet. *39*, 397–402.

Field, H.A., Dong, P.D., Beis, D., et al. (2003a). Formation of the digestive system in zebrafish. II. Pancreas morphogenesis. Dev. Biol. *261*, 197–208.

Field, H.A., Ober, E.A., Roeser, T., et al. (2003b). Formation of the digestive system in zebrafish. I. Liver morphogenesis. Dev. Biol. *253*, 279–290.

Flores, M.V., Hall, C.J., Davidson, A.J., et al. (2008). Intestinal differentiation in zebrafish requires Cdx1b, a functional equivalent of mammalian Cdx2. Gastroenterology *135*, 1665–1675.

Gao, C., Zhu, Z., Gao, Y., et al. (2018). Hepatocytes in a normal adult liver are derived solely from the embryonic hepatocytes. J. Genet. Genomics *45*, 173–175.

Goessling, W., and Stainier, D.Y. (2016). Endoderm specification and liver development. Methods Cell Biol. *134*, 463–483.

Gong, L., Gong, H., Pan, X., et al. (2015). p53 isoform Δ113p53/Δ133p53 promotes DNA double-strand break repair to protect cell from death and senescence in response to DNA damage. Cell Res. *25*, 351–369.

Goodings, C., Smith, E., Mathias, E., et al. (2015). Hhex is required at multiple stages of adult hematopoietic stem and progenitor cell differentiation. Stem Cells *33*, 2628–2641.

Guan, Y., Huang, D., Chen, F., et al. (2016). Phosphorylation of Def regulates Nucleolar p53 turnover and cell cycle progression through Def recruitment of Calpain3. PLoS Biol. *14*, e1002555.

Hallaq, H., Pinter, E., Enciso, J., et al. (2004). A null mutation of Hhex results in abnormal cardiac development, defective vasculogenesis and elevated Vegfa levels. Development *131*, 5197–5209.

He, J., Lu, H., Zou, Q., et al. (2014). Regeneration of liver after extreme hepatocyte loss occurs mainly via biliary transdifferentiation in zebrafish. Gastroenterology *146*, 789–800.e8.

Her, G.M., Chiang, C.C., Chen, W.Y., et al. (2003). In vivo studies of liver-type fatty acid binding protein (L-FABP) gene expression in liver of transgenic zebrafish (Danio rerio). FEBS Lett. *538*, 125–133.

Hromas, R., Radich, J., and Collins, S. (1993). PCR cloning of an orphan homeobox gene (PRH) preferentially expressed in myeloid and liver cells. Biochem. Biophys. Res. Commun. *195*, 976–983.

Huang, H., Ruan, H., Aw, M.Y., et al. (2008). Mypt1-mediated spatial positioning of Bmp2-producing cells is essential for liver organogenesis. Development *135*, 3209–3218.

Hunter, M.P., Wilson, C.M., Jiang, X., et al. (2007). The homeobox gene Hhex is essential for proper hepatoblast differentiation and bile duct morphogenesis. Dev. Biol. *308*, 355–367.

Kikuchi, Y., Agathon, A., Alexander, J., et al. (2001). Casanova encodes a novel Sox-related protein necessary and sufficient for early endoderm formation in zebrafish. Genes Dev. *15*, 1493–1505.

Kimmel, R.A., Onder, L., Wilfinger, A., et al. (2011). Requirement for Pdx1 in specification of latent endocrine progenitors in zebrafish. BMC Biol. *9*, 75.

Kubo, A., Kim, Y.H., Irion, S., et al. (2010). The homeobox gene Hex regulates hepatocyte differentiation from embryonic stem cell-derived endoderm. Hepatology *51*, 633–641.

Liu, Y., Kaneda, R., Leja, T.W., et al. (2014). Hhex and Cer1 mediate the Sox17 pathway for cardiac mesoderm formation in embryonic stem cells. Stem Cells *32*, 1515–1526.

Manfroid, I., Ghaye, A., Naye, F., et al. (2012). Zebrafish sox9b is crucial for hepatopancreatic duct development and pancreatic endocrine cell regeneration. Dev. Biol. *366*, 268–278.

Ober, E.A., Field, H.A., and Stainier, D.Y. (2003). From endoderm formation to liver and pancreas development in zebrafish. Mech. Dev. *120*, 5–18.

Ober, E.A., Verkade, H., Field, H.A., et al. (2006). Mesodermal Wnt2b signalling positively regulates liver specification. Nature *442*, 688–691.

Paz, H., Lynch, M.R., Bogue, C.W., et al. (2010). The homeobox gene Hhex regulates the earliest stages of definitive hematopoiesis. Blood *116*, 1254–1262.

Rankin, S.A., Kormish, J., Kofron, M., et al. (2011). A gene regulatory network controlling hhex transcription in the anterior endoderm of the organizer. Dev. Biol. *351*, 297–310.

Shields, B.J., Jackson, J.T., Metcalf, D., et al. (2016). Acute myeloid leukemia requires Hhex to enable PRC2-mediated epigenetic repression of Cdkn2a. Genes Dev. *30*, 78–91.

Shih, H.P., Wang, A., and Sander, M. (2013). Pancreas organogenesis: from lineage determination to morphogenesis. Annu. Rev. Cell Dev. Biol. *29*, 81–105.

Soufi, A., and Jayaraman, P.S. (2008). PRH/Hex: an oligomeric transcription factor and multifunctional regulator of cell fate. Biochem. J. *412*, 399–413.

Tao, T., and Peng, J. (2009). Liver development in zebrafish (Danio rerio). J. Genet. Genomics *36*, 325–334.

Wallace, K.N., Yusuff, S., Sonntag, J.M., et al. (2001). Zebrafish hhex regulates liver development and digestive organ chirality. Genesis *30*, 141–143.

Wang, Y., Zhu, Q., Huang, L., et al. (2016). Interaction between Bms1 and Rcl1, two ribosome biogenesis factors, is evolutionally conserved in zebrafish and human. J. Genet. Genomics *43*, 467–469.

Watanabe, H., Takayama, K., Inamura, M., et al. (2014). HHEX promotes hepatic-lineage specification through the negative regulation of eomesodermin. PLoS One *9*, e90791.

Williams, H., Jayaraman, P.S., and Gaston, K. (2008). DNA wrapping and distortion by an oligomeric homeodomain protein. J. Mol. Biol. *383*, 10–23.

Xu, J., Cui, J., Del Campo, A., et al. (2016). Four and a half LIM domains 1b (Fhl1b) is essential for regulating the liver versus pancreas fate decision and for β-cell regeneration. PLoS Genet. *12*, e1005831.

Yang, S.L., Aw, S.S., Chang, C., et al. (2011). Depletion of Bhmt elevates sonic hedgehog transcript level and increases β-cell number in zebrafish. Endocrinology *152*, 4706–4717.

Yee, N.S., Yusuff, S., and Pack, M. (2001). Zebrafish pdx1 morphant displays defects in pancreas development and digestive organ chirality, and potentially identifies a multipotent pancreas progenitor cell. Genesis *30*, 137–140.

Zaret, K.S. (2008). Genetic programming of liver and pancreas progenitors: lessons for stem-cell differentiation. Nat. Rev. Genet. *9*, 329–340.

Zhang, D., Golubkov, V.S., Han, W., et al. (2014). Identification of Annexin A4 as a hepatopancreas factor involved in liver cell survival. Dev. Biol. *395*, 96–110.

Zhang, W., Yatskievych, T.A., Cao, X., et al. (2002). Regulation of Hex gene expression by a Smads-dependent signaling pathway. J. Biol. Chem. *277*, 45435–45441.

Zhao, H., Han, D., Dawid, I.B., et al. (2012). Homeoprotein hhex-induced conversion of intestinal to ventral pancreatic precursors results in the formation of giant pancreata in Xenopus embryos. Proc. Natl Acad. Sci. USA *109*, 8594–8599.